GaN nanowire lasers with low lasing thresholds

Silvija Gradečak, Fang Qian, Yat Li, Hong-Gyu Park, and Charles M. Lieber[a)]
Harvard University, Cambridge, Massachusetts 02138

(Received 8 August 2005; accepted 16 September 2005; published online 18 October 2005)

We report optically pumped room-temperature lasing in GaN nanowires grown by metalorganic chemical vapor deposition (MOCVD). Electron microscopy images reveal that the nanowires grow along a nonpolar ⟨11-20⟩ direction, have single-crystal structures and triangular cross sections. The nanowires function as free-standing Fabry–Pérot cavities with cavity mode spacings that depend inversely on length. Optical excitation studies demonstrate thresholds for stimulated emission of 22 kW/cm^2 that are substantially lower than other previously reported GaN nanowires. Key contributions to low threshold lasing in these MOCVD GaN nanowire cavities and the development of electrically pumped GaN nanowire lasers are discussed. © *2005 American Institute of Physics*. [DOI: 10.1063/1.2115087]

Semiconductor nanowires are emerging as versatile nanoscale building blocks for the assembly of photonic devices,[1,2] including polarization sensitive photodetectors,[3] light-emitting diodes,[4–7] and lasers.[8–11] For example, single nanowires have been shown to function as optical waveguides and Fabry–Pérot cavities,[9,10] and the optical excitation of single nanowire cavities has produced stimulated emission and lasing.[8,9,11] Integrated applications exploiting nanowire lasers will likely involve electrical injection devices, yet electrically driven lasing has only been obtained from CdS nanowire-based devices to date.[10]

To develop nanowires injection lasers as general sources with outputs covering a broad range of the electromagnetic spectrum requires efficient strategies for electron-hole injection and optimization of cavity properties and lasing thresholds in materials where the bandgap can be readily varied. Planar light-emitting and laser diode structures based on aluminum–gallium–indium nitride (AlGaIn)N alloys[12] suggest that this material system could be ideal for developing wavelength tunable nanowire injection lasers. Indeed, we have recently demonstrated that *n*-GaN/InGaN/*p*-GaN core/shell/shell radial nanowire heterostructures can be prepared and configured as light-emitting diodes, where the emission wavelength is defined by the InGaN shell.[6] These nanowire heterostructures exhibited poor waveguiding/cavity properties, which has hindered the observation of stimulated emission and lasing. In addition, optically pumped lasing in GaN nanowires has been reported,[9] although the estimated thresholds are substantially larger than observed in either CdS or ZnO nanowires.[8,10] Here, we report new optical studies of GaN nanowires grown by metalorganic chemical vapor deposition (MOCVD) that address this critical issue of the cavity, and show that through control of growth it is possible to achieve low threshold lasing.

Our GaN nanowires were grown by MOCVD on sapphire substrates using trimethylgallium and ammonia as Ga and N precursors, respectively, silane as the *n*-type dopant, and hydrogen as a carrier gas, as described previously.[6] Two distinct classes of nanowires were prepared, depending on their growth temperatures: "Low-temperature" (LT) and "high-temperature" (HT) nanowires were synthesized at 775 and 950 °C, respectively. Here, we concentrate on HT nanowires due to their superior morphology, while results on LT nanowires are briefly discussed for comparison.

High-resolution transmission electron microscopy (TEM) images of a typical HT nanowire [Fig. 1(a)] reveal a single-crystal wurtzite structure. A selected-area diffraction pattern recorded along the [0001] zone axis [inset, Fig. 1(a)] shows that MOCVD GaN nanowires grow along a nonpolar ⟨11-20⟩ direction. This growth direction was confirmed for all (~100) nanowires examined by TEM. Scanning electron

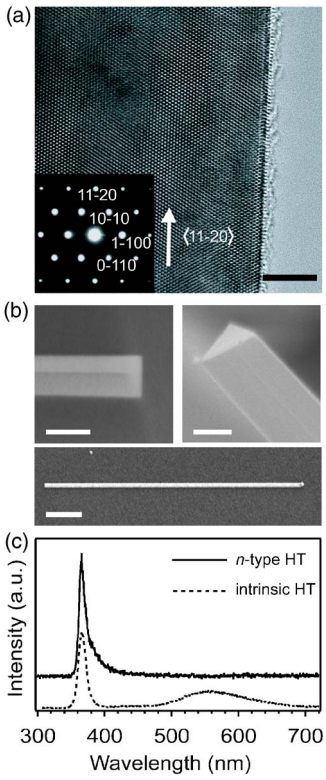

FIG. 1. (a) High-resolution TEM image of an *n*-type HT MOCVD GaN nanowire along [0001] zone axis (scale bar, 5 nm) and corresponding diffraction pattern indicating ⟨11-20⟩ nanowire growth direction. (b) SEM images of HT nanowires revealing their morphological properties: naturally cleaved end facet (the upper left-hand image; scale bar, 200 nm), triangular cross section (the upper right-hand image; scale bar, 200 nm), and uniform diameter (the lower image; scale bar, 2 μm). (c) PL spectra of *n*-type and intrinsic HT nanowires with excitation power density of 3 kW/cm^2.

[a)]Electronic mail: cml@cmliris.harvard.edu

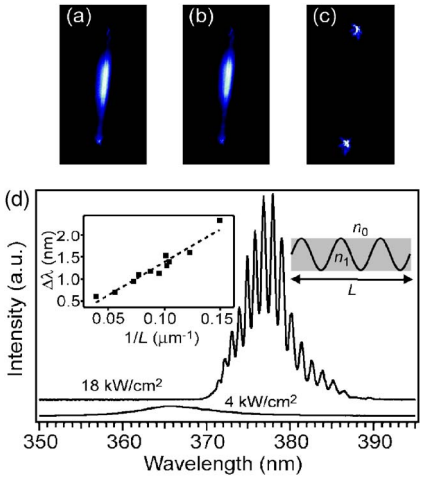

FIG. 2. (Color) Power-dependent PL studies of *n*-type HT GaN nanowire cavity properties. Images of a single nanowire excited with (a) 4 kW/cm^2, (b) 17 kW/cm^2, and (c) 66 kW/cm^2. (d) PL spectra recorded at the end of 13 μm long nanowire for 4 kW/cm^2 and 18 kW/cm^2 power densities showing Fabry–Pérot cavity modes with average mode spacing of 1.1 nm. Right inset, schematic representation of a longitudinal nanowire cavity with length L whose index of refraction, n_1, is larger than that of surrounding air, n_0. Left inset, mode spacing vs inverse nanowire length.

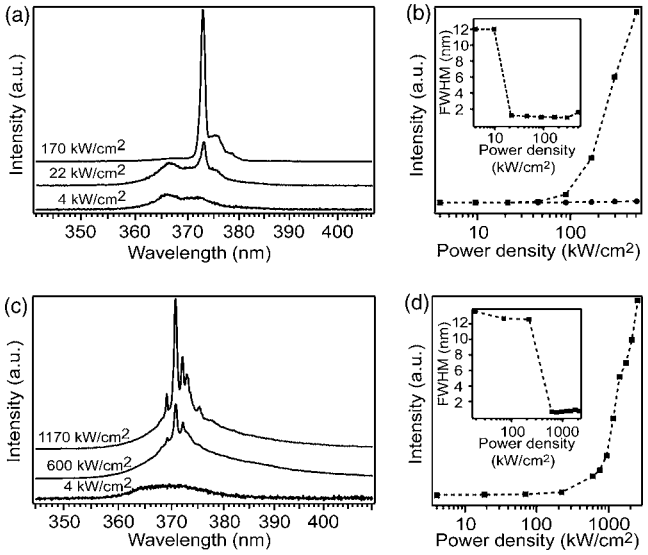

FIG. 3. (a) PL spectra of *n*-type HT nanowire recorded at 4, 22, and 170 kW/cm^2 excitation power densities. Spectra are offset for clarity. (b) Intensity of the 373 nm lasing peak (squares) and 365 nm spontaneous peak (circles) vs power density for the same nanowire. Inset, FWHM of the lasing peak vs power density. Solid symbols correspond to experimental data and dashed lines are guides for the eyes. (c) and (d) Same as above for *n*-type LT nanowire. Spectra were recorded at 4, 600, and 1170 kW/cm^2 and intensity vs power density was measured for lasing peak at 371 nm.

microscopy (SEM) images also show that the nanowires have triangular cross sections [Fig. 1(b), top] with diameters of 100–300 nm. The HT nanowires have very uniform thicknesses (i.e., are not tapered) and smooth surfaces over lengths up to 100 μm [Fig. 1(b), bottom], although our optical studies were carried out on nanowires with typical lengths between 10 and 30 μm. The uniform thickness and smooth surface morphology of these HT nanowires is important for waveguiding without large losses from surface emission. Last, the SEM images demonstrate that the nanowires have sharp cleaved end facets [Fig. 1(b), top], which can be attributed to the sonication process used to remove nanowires from the growth substrate,[10] required for a good cavity.

Optical studies of individual GaN nanowires were carried out using a home-built far-field epifluorescence apparatus[13] using a *Q*-switched $Nd:YVO_4$ laser (266 nm, 35 kHz repetition rate, and 7 ns pulse duration) as the excitation source. Photoluminescence (PL) spectra of *n*-type HT GaN nanowires acquired at low excitation intensity [Fig. 1(c)] show sharp 12 nm full width at half maximum (FWHM) spontaneous emission centered at 365 nm (3.40 eV), corresponding to GaN bandedge emission.[14] Significantly, the PL data acquired from these *n*-type HT GaN nanowires are free from deep-level yellow emission. In contrast, intrinsic HT GaN nanowires prepared in a similar manner [Fig. 1(c)] exhibit a broad band centered at ≈550 nm (2.26 eV). These observations agree with measurements of GaN thin films in which yellow to ultraviolet luminescence ratio decreases with Si doping[15] and indicates excellent optical properties of *n*-type HT GaN nanowires. Moreover, overall integrated luminescence intensity obtained under identical excitation conditions increases for *n*-type versus intrinsic nanowires.

The cleaved end facets of the nanowires can define a longitudinal nanowire resonant cavity,[9,10] analogous to cleaved facets in planar structures.[16] At low excitation power densities, I_p, spontaneous emission was observed from both the body and ends of HT GaN nanowires [Fig. 2(a)]. With increasing I_p, the emission intensity at nanowire ends increases [Fig. 2(b)] and becomes dominant as shown in Fig. 2(c), thus indicating strong waveguiding properties. Significantly, a spectral analysis of the emission from the nanowire ends at higher excitation densities exhibits a redshift with well-defined periodic variation in the intensity [Fig. 2(d)] that are indicative of Fabry–Pérot cavity modes. The mode spacing $\Delta\lambda$ for a cavity with length L is given by[17] $\Delta\lambda=\lambda^2/[2L(n-\lambda(dn/d\lambda))]$, where n is GaN index of refraction and $dn/d\lambda$ is the first-order dispersion of the index of refraction (for $\lambda=378$ nm,[18] $n=2.64$, and $dn/d\lambda=-0.0077\ nm^{-1}$). For most of our nanowires, their lengths scale with corresponding mode spacings according to the equation [inset, Fig. 2(d)].

The estimated quality factor, Q, of these *n*-type GaN nanowire cavities is in the 500–700 range, where $Q=\lambda/\Delta\lambda$ and $\Delta\lambda$ is the FWHM of the cavity mode. The actual Q could be higher since the $\Delta\lambda$'s are comparable to the spectrometer resolution. To analyze quantitatively the nanowire cavity and effect of the triangular cross section, we performed three-dimensional finite-difference time-domain (FDTD) calculations[19] for free-standing triangular and cylindrical GaN nanowires with the same cross-sectional area and length. Both geometries have modes with quality factors of 1000–1500, that are higher than estimated from experimental data or macroscopic models[16] that do not account for the finite size of the nanowire. Interestingly, these calculations also indicate better wavelength stability of quality factors for triangular versus cylindrical nanowires, which could be especially important in future applications where wavelength tunability is desirable.

Figures 3(a) and 3(b) show the results of optically excited lasing in a 25 μm long *n*-type HT GaN nanowire. At low I_p's, spontaneous emission was centered around 365 nm [Fig. 3(a)]. Above the threshold power density of $I_p\sim 22\ kW/cm^2$, a narrow peak (<0.8 nm FWHM, limited

by the spectral resolution of the detection system) developed at 373 nm (3.33 eV). The intensity of this peak increased superlinearly above the threshold with an intensity $\propto I_p^{2.02}$, while the dependence of spontaneous peak intensity is sublinear, $\propto I_p^{0.59}$ [Fig. 3(b)]. The simultaneous line narrowing and superlinear increase of intensity at pump densities as low as 22 kW/cm^2 represents, to our knowledge, the lowest room-temperature lasing threshold reported for GaN materials, and is comparable to that of CdS nanowires which have been already used for realization of the first single-nanowire electrically driven laser.[10]

For comparison, we also investigated other types of GaN nanowires. For example, Figures 3(c) and 3(d) show results of the lowest measured I_p threshold in a LT GaN nanowire, which were previously utilized for core/shell nanowire light-emitting diodes.[6] In this 6 μm long nanowire, lasing was evidenced by the appearance of several narrow, FWHM <0.8 nm, lines and a concurrent superlinear increase in the peak intensity at $I_p \geqslant 600$ kW/cm^2. Measurements made on a number of distinct *n*-type HT and LT nanowires showed that *n*-type HT nanowires have systematically at least an order of magnitude lower lasing thresholds than *n*-type LT nanowires. In addition, these HT *n*-type nanowires had lasing thresholds several times lower than intrinsic HT nanowires and *n*-type GaN nanowires grown by chemical vapor deposition[5] with polar $\langle 0001 \rangle$ growth direction.

Several factors are believed to contribute to the low threshold power density for stimulated emission in *n*-type HT GaN nanowires, including: (a) Excellent structural and morphological properties, (b) nonpolar growth direction, and (c) Si doping. The nanowires are free from dislocations, which can lead to nonradiative recombination,[20] due to virtually substrate-free growth mechanism. The dislocation-free structure of the nanowires represents a general advantage compared to planar GaN devices. The HT nanowires also have more uniform diameters than LT nanowires, and this morphological uniformity will in general yield superior cavity properties. In addition, the cavity in the triangular cross section nanowire is formed along a nonpolar $\langle 11\text{-}20 \rangle$ direction, and consequently is expected to have a higher optical gain.[21] Our FDTD calculations have further shown that the triangular cross section nanowires have more uniformly high-Q factors for a wide range of wavelengths than near-cylindrical hexagonal nanowires with a $\langle 0001 \rangle$ growth direction,[22] and thus indicates that $\langle 11\text{-}20 \rangle$ nanowires will be best for tunable laser sources. Last, Si doping leads to a reduction in deep-level emission, which would otherwise increase the threshold. At the same time, this suggests that the Si-doped *n*-type HT GaN nanowires will be an ideal starting point from which to design electrical injection lasers based, for example, on a core (*n*-type GaN nanowire) multishell architecture.[6]

In summary, we have studied optically pumped lasing in MOCVD GaN nanowires with a nonpolar $\langle 11\text{-}20 \rangle$ growth direction. These nanowires form natural free-standing Fabry–Pérot cavities with triangular cross sections, dislocation-free structures, and uniform diameters. These structural characteristics lead to excellent cavity properties, and together with *n*-type doping, are crucial for reducing the excitation power density required for stimulated emission. Significantly, the lowest recorded threshold density was only 22 kW/cm^2, which makes *n*-type MOCVD GaN nanowires ideal candidates for electrically driven nanowire lasers based on our radial core/multishell architecture.

The authors thank R. Agarwal and C. J. Barrelet for helpful discussions and technical help. Two of the authors (S. G. and Y. L.) acknowledge the Swiss National Science Foundation and Croucher Foundation, respectively, for fellowship support. We thank the Air Force of Scientific Research and Defense Advanced Research Projects Agency for support of this work, and Thomas-Swan Scientific Equipment, Ltd. for support of the MOCVD system.

[1] C. M. Lieber, MRS Bull. **28**, 486 (2003).
[2] P. Yang, MRS Bull. **30**, 85 (2005).
[3] J. Wang, M. S. Gudiksen, X. Duan, Y. Cui, and C. M. Lieber, Science **293**, 1455 (2001).
[4] X. Duan, Y. Huang, Y. Cui, J. Wang, and C. M. Lieber, Nature (London) **409**, 66 (2001).
[5] Z. Zhong, F. Qian, D. Wang, and C. M. Lieber, Nano Lett. **3**, 343 (2003).
[6] F. Qian, Y. Li, S. Gradečak, D. Wang, C. J. Barrelet, and C. M. Lieber, Nano Lett. **4**, 1975 (2004).
[7] Y. Huang, X. Duan, and C. M. Lieber, Small **1**, 142 (2005).
[8] M. H. Huang, S. Mao, H. Feick, H. Yan, Y. Wu, H. Kind, E. Weber, R. Russo, and P. Yang, Science **292**, 1897 (2001).
[9] J. C. Johnson, H. J. Choi, K. P. Knutsen, R. D. Schaller, P. Yang, and R. J. Saykally, Nat. Mater. **1**, 106 (2002).
[10] X. Duan, Y. Huang, R. Agarwal, and C. M. Lieber, Nature (London) **421**, 241 (2003).
[11] R. Agarwal, C. J. Barrelet, and C. M. Lieber, Nano Lett. **5**, 917 (2005).
[12] S. Nakamura, S. Pearton, and G. Fasol, *The Blue Laser Diode: The Complete Story* (Springer, Berlin, 2000).
[13] M. S. Gudiksen, L. L. Lauhon, J. Wang, D. C. Smith, and C. M. Lieber, Nature (London) **415**, 617 (2002).
[14] R. Pässler, Phys. Status Solidi B **216**, 975 (1999).
[15] H. C. Yang, T. Y. Lin, M. Y. Huang, and Y. F. Chen, J. Appl. Phys. **86**, 6124 (1999).
[16] O. Svelto, *Principles of Lasers* (Plenum, New York, 1998).
[17] J. J. Song and W. C. Wang, J. Appl. Phys. **55**, 660 (1984).
[18] N. Antoine-Vincent, F. Natali, M. Mihailovic, A. Vasson, J. Leymaire, P. Disseix, D. Byrne, F. Semond, and J. Massies, J. Appl. Phys. **93**, 5222 (2003).
[19] B. J. Li and P. L. Liu, IEEE J. Quantum Electron. **32**, 1583 (1996).
[20] S. Nakamura, Science **281**, 956 (1998).
[21] E. Kuokstis, C. Q. Chen, J. W. Yang, M. Shatalov, M. E. Gaevski, V. Adivarahan, and M. A. Khan, Appl. Phys. Lett. **84**, 2998 (2004).
[22] T. Kuykendall, P. J. Pauzauskie, Y. Zhang, J. Goldberger, D. Sirbuly, J. Denlinger, and P. Yang, Nat. Mater. **3**, 524 (2004).